Environ Geol (2009) 58:521–529
DOI 10.1007/s00254-008-1527-2

ORIGINAL ARTICLE

Combining TEM/resistivity joint inversion and magnetic data for groundwater exploration: application to the northeastern part of Greater Cairo, Egypt

Sultan Awad Sultan · Fernando Monteiro Santos

Received: 27 March 2008 / Accepted: 20 August 2008 / Published online: 20 September 2008

Abstract This paper presents the combination of two complementary methods, magnetic and joint inversion of resistivity/TEM data, as an effective approach to characterize groundwater reservoirs. Twenty stations of transient electromagnetic (TEM) and vertical electrical soundings (VES) were measured and interpreted using a joint inversion technique to evaluate the subsurface low resistivity zones connected to the groundwater reservoir. A complementary survey including 871 land magnetic stations was carried out at the same area to detect the upper surface of the basaltic sheet, which represents the bottom of the Miocene aquifer in the study area. The geological log from one borehole drilled in the zone was used to partially calibrate the calculated models. The results revealed that the study area consists of five different geological units with ages ranging from Paleogene (Oligocene) to Quaternary. The methodology provides good results at a very low cost when compared with drilling boreholes.

Keywords Electromagnetic · Resistivity · Magnetic · Joint inversion · Groundwater

S. A. Sultan (✉)
National Research Institute of Astronomy and Geophysics,
Helwan, Cairo 11722, Egypt
e-mail: sultan_awad@yahoo.com

S. A. Sultan · F. M. Santos
Universidade de Lisboa and Centro de Geofísica da
Universidade de Lisboa-IDL, Campo Grande,
Ed. C8, 1749-016 Lisbon, Portugal
e-mail: fasantos@fc.ul.pt

Introduction

Electrical and electromagnetic geophysical methods have been widely used in engineering, mining and groundwater investigations because of good correlation between electrical properties of the rocks and fluid content of geological formations (Flathe 1955; Zohdy 1969; Fitterman and Stewart 1986; McNeill 1990). Among the various geophysical methods, the direct current (DC) or resistivity method is probably the most popular in groundwater studies due to the simplicity of the technique, easy interpretation of the data and rugged nature of the associated instrumentation. The technique is widely used in soft and hard rock areas (e.g., Van Overmeeren 1989; Urish and Frohlich 1990; Ebraheem et al. 1997). The transient electromagnetic (TEM) method is relatively new. It has been developed more intensively since the mid-1980 and has been commonly used in environmental and hydrogeological investigation (Meju 2005 and Goldman et al. 1994). It is well known that DC soundings are quite sensitive to resistive layers and structures imbedded in section and sensitive to conductive layers. The TEM shows a complementary behavior because it is very sensitive to conductive layers and insensitive to resistive ones (Barsukov et al. 2004). However, those methods suffer from equivalence problem: different models can produce almost identical responses. It is very difficult to distinguish between models with layers of similar transverse resistance, $T = r \times t$ where r and t are the resistivity and thickness of a thin resistive layer within a conductive host, and models with layers of similar longitudinal conductance, $S = t/r$, where now the thin conductive bed is within a resistive host. These are called T and S equivalence, respectively. Goldman et al. (1994) considered two types of equivalence: M-equivalence and E-equivalence. M-

equivalence results from the non-uniqueness in choosing a model for the specific observation system used in the experiment. E-equivalence is caused by the inherent properties of experimental data such as external noise, instrument accuracy, etc. As a result, one must consider experimental data as belonging to certain confidence regions. Different data sets within the limits of the same region can be fitted with responses from different (equivalent) models.

Several authors have used joint inversion of TEM and vertical electrical soundings (VES) data in order to decrease the ambiguity inherited to each method (Meju 2005; Sharma and Baranwal 2005). Joint DC and TEM 1D inversion allows defining parameters of well and poorly conducting layers of section where DC and TEM separately, rather often, do not let to make that (Barsukov et al. 2004).

In this study, we used joint inversion of DC VES and TEM data to defined stratigraphic units and hydrogeological characteristics of an aquifer. The depth of the deep basaltic sheet on the study area estimated by those methods was compared favorably with the results obtained from the interpretation of a land magnetic survey carried out at the same area, through the map of the top of the basaltic sheet (Fig. 1).

Geology of the area

The survey area lies at the northeastern part of Greater Cairo (Egypt) and is located between latitudes 30°09′ and 30°22′ N and longitudes 31°22′ and 31°37′ E (Fig. 2). Most part of the geological units in the study area belong to the Quaternary, Middle Miocene and Oligocene deposits. The Quaternary deposits are represented by different formations such as sand sheets which are located at the eastern part of the area. Inshas formation occupying the northern and eastern part of the study area consists of cross-bedded sand, intercalated with Nile mud and silt. Bilbies formation is located at the central and eastern parts of the area and is made up of medium to coarse-grained and cross-bedded sands with plant roots and carbonate pockets. El Debba formation, in the southern part of the area, consists of coarse-grained sands intercalated with flint. The Middle Miocene is represented by Hommath formation, which is located at the central part of the survey area and made up of interbedded yellow sandy limestone, sandstone and sandy marl. The Oligocene deposits are represented by Gabal Ahmar Formation, which is composed of sand and sandstone according to EGSMA (1998) (Fig. 3).

Figure 4 shows the subsurface stratigraphy as described from a 202 m deep borehole drilled at the eastern part of the survey area by EGSMA (1998). The stratigraphic column consists of Quaternary, Middle Miocene and Oligocene deposits. The Quaternary deposits are represented by sand

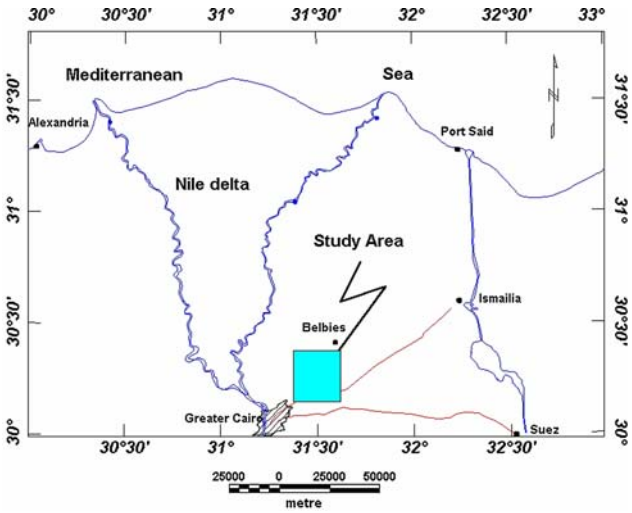

Fig. 1 Location map of the study area

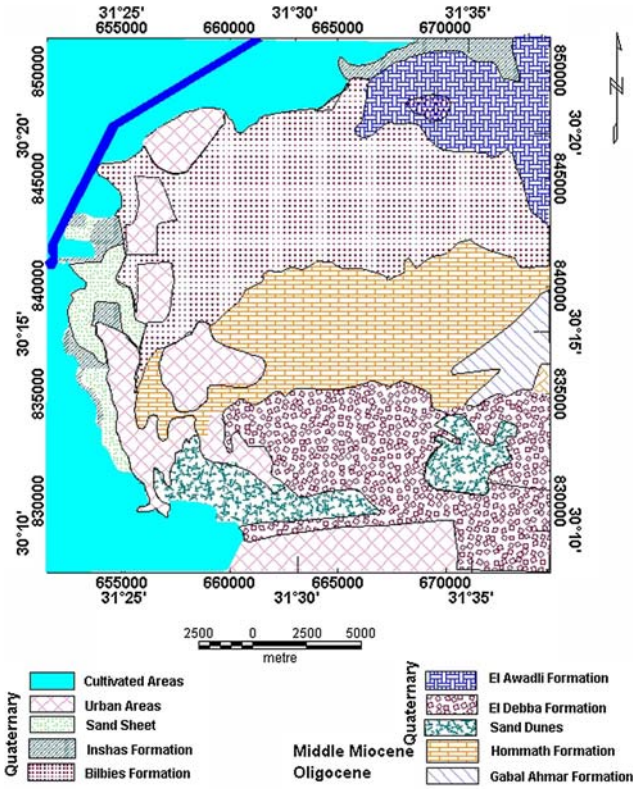

Fig. 2 Geological map of the study area (Modified after EGSMA 1998)

sheet and the Middle Miocene is represented by the Hommath formation. The Oligocene deposits are represented by Gabal Ahmar Formation (sand and sandstone) and by a Basaltic sheet lying between 113.5 m (top) and 162.2 m (bottom) depths. The analysis of rock samples from the basaltic sheet indicates that its top and bottom are altered

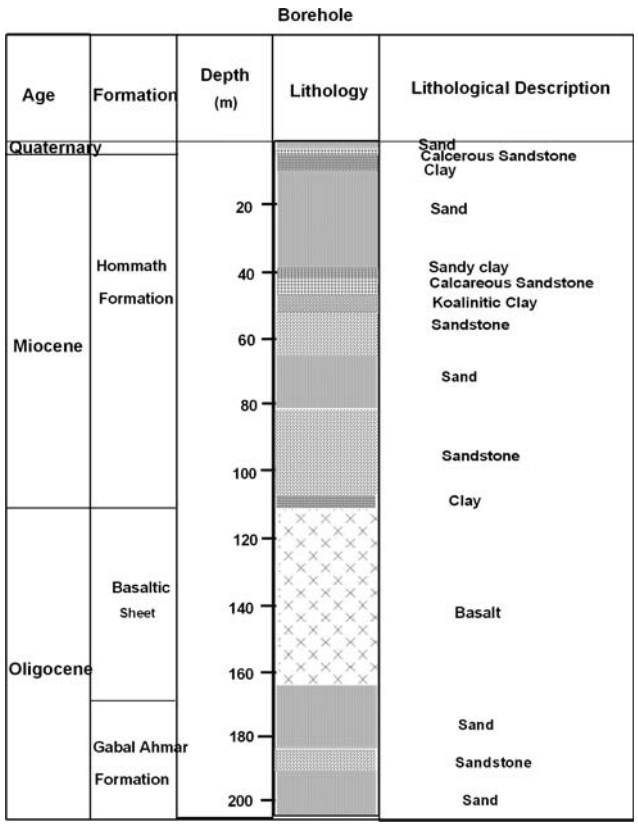

Fig. 3 Geological log from the borehole drilled by EGSMA (1998)

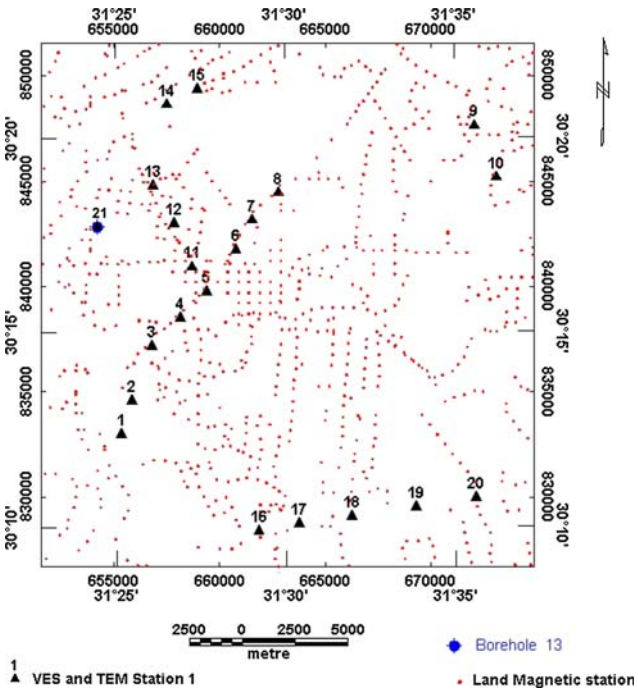

Fig. 4 Location map of the geophysical measurements

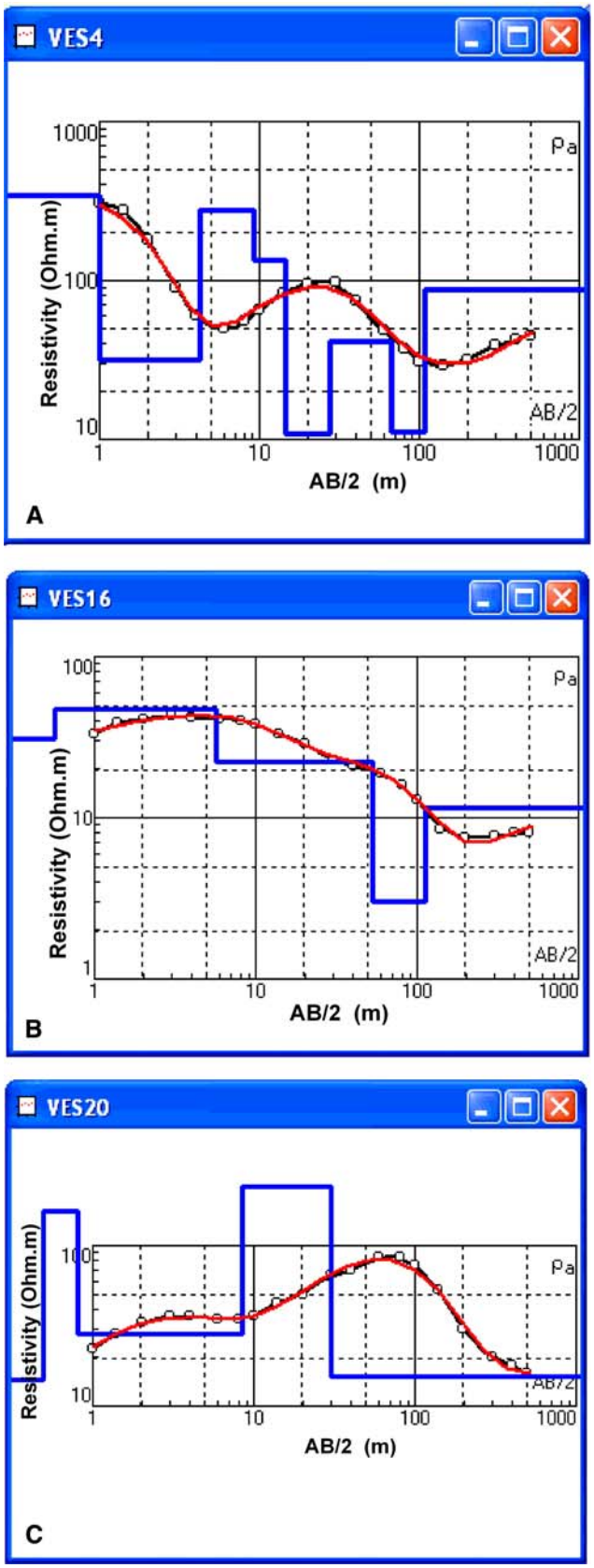

Fig. 5 Data and interpretation of three vertical electrical soundings, VES 4 (A), 16 (B) and 20 (C). RMS of 6, 4 and 4%, respectively

and fractured. Also, the hydrochemistry of the water samples from the borehole indicate that the total dissolved salt (TDS) is 2,000 ppm and electrical conductivity is 1,250 μS/cm suggesting that water has low ionic content.

Geophyiscal measurements and interpretation

The geophysical measurements carried out in this work included 20 VES and TEM soundings and 871 land magnetic stations. Figure 5 shows the location of the measuring sites.

Vertical electrical sounding

The VES were undertaken with current electrodes separation ranging from 2 to 1,000 m, i.e., distance AB/2 varying from 1 to 500 m. The data were acquired using a SYSCAL–R2 resistivity meter. The apparent resistivity data acquired at each site was inverted using the IPI2win software (IPI2Win-1D Program 2000). Figure 6 shows three examples of apparent resistivity curves and its inversions.

It was noted that there are a strong correlation between resistivity and thickness of some layers. For example, it was found significant direct and reverse correlation for the resistivity (r) and thickness (t) at sounding VES 16 where the best fitting fulfills for thickness values ranging from 0.3 to 0.88 m and for resistivity values ranging from 20 to 35 ohm-m (direct correlation) for first layer. In the second layer, there is a reverse correlation between thickness and resistivity where the best fitting fulfills for resistivity values between 45 and 50 ohm-m and thickness values between 4.3 and 5.7 m. At the third layer the resistivity values can vary from 21 to 24 ohm-m and the thickness from 44 to 52 m. There is also a direct correlation between resistivity and thickness (Fig. 7) in the fourth layer.

VES station 21 was measured in the vicinity of a borehole in order to correlate the resistivity values with geological information (Fig. 8). However, no TEM measurements was carried out around the borehole and the VES 21 due to power lines of high voltages located near the borehole. The calculated models exhibit in general four geoelectrical units representing the shallow section in the study area. These units correlate from the top to bottom with the Quaternary deposits, the Miocene deposits, the Miocene aquifer, the Basaltic sheet and the Oligocene

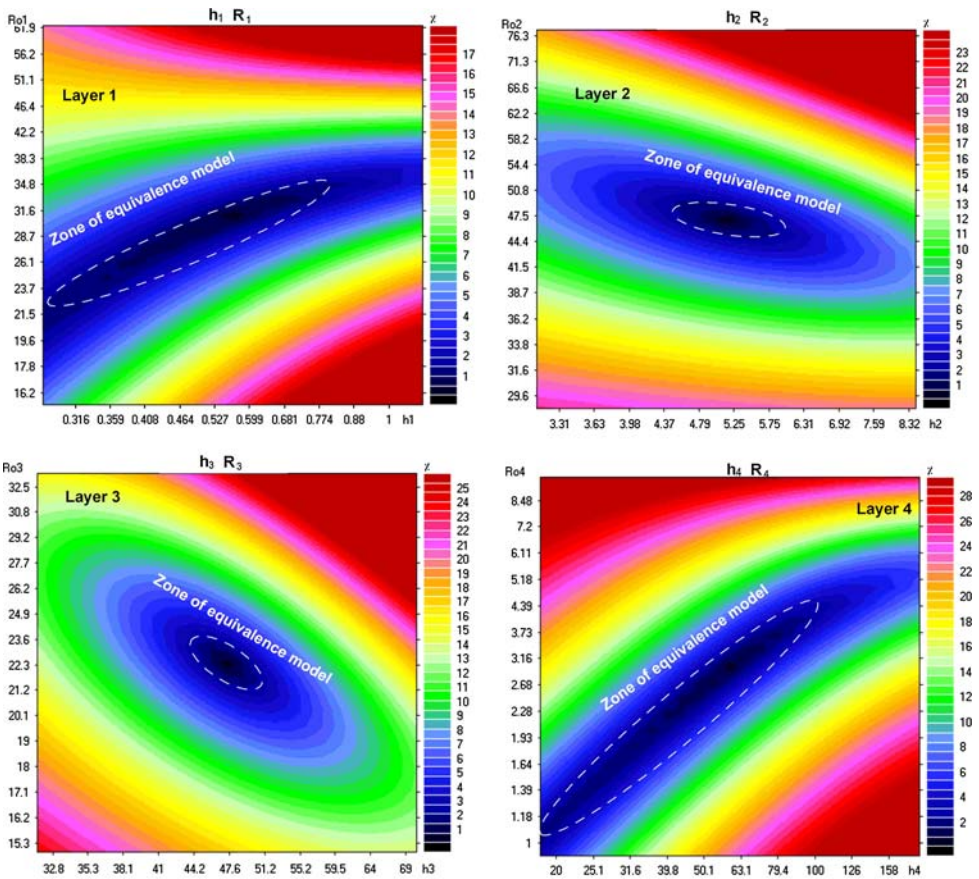

Fig. 6 Parameter space for four layers of the model of sounding VES 16, the dark color (*black*) refers to best fitting with minimum error

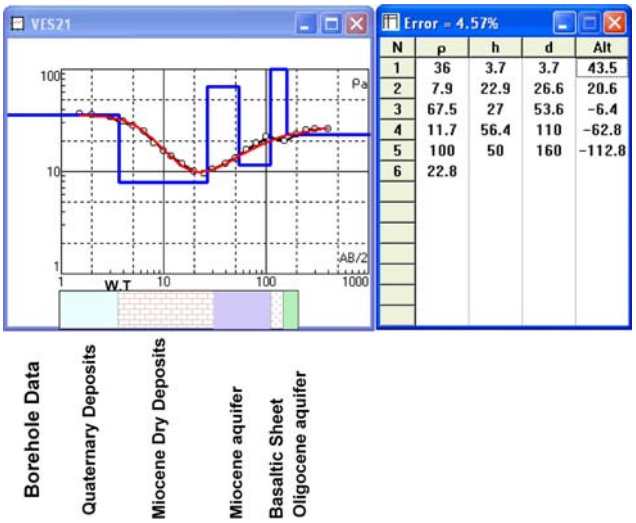

Fig. 7 Interpretation of VES21 compare with borehole data

aquifer. The deepest layers, the Basaltic sheet and the Oligocene aquifer, were only sampled at a few soundings. Due to the equivalence problem the geoelectrical parameters of some layers are not very well determined.

Transient electromagnetic

The TEM measurements were carried out using the SIROTEM-3 instrument with a coincident configuration. 50×50 m^2 transmitter/receiver loops were used. The data was inverted assuming layered models and using the TEMIX/XL version 4 software (Interpex Limited 1995). Figure 9 show examples of the apparent resistivity curve and the result of its inversion. In general the TEM soundings were inverted assuming four layer models. A better resolution of the low resistivity layers is expected, relatively to high resistivity ones.

Joint inversion of VES and TEM data

It is well known that the presence of small-scale heterogeneities near the ground surface at a sounding position may cause DC resistivity sounding curves to be distorted—an effect known as static-shift—(e.g., Barker 1981) and, if unaccounted for, it will lead to erroneous interpretations. Since the data in the TEM method are obtained considering only the magnetic field (the secondary one), they are not affected by the presence of electric charges in the surfaces of such small structures and are free of static-shift effect. For this reason, the VES apparent resistivity curves were first compared with the TEM apparent resistivity curves in order to evaluate the distortion effect. To perform such comparison, the time in TEM curves was converted into

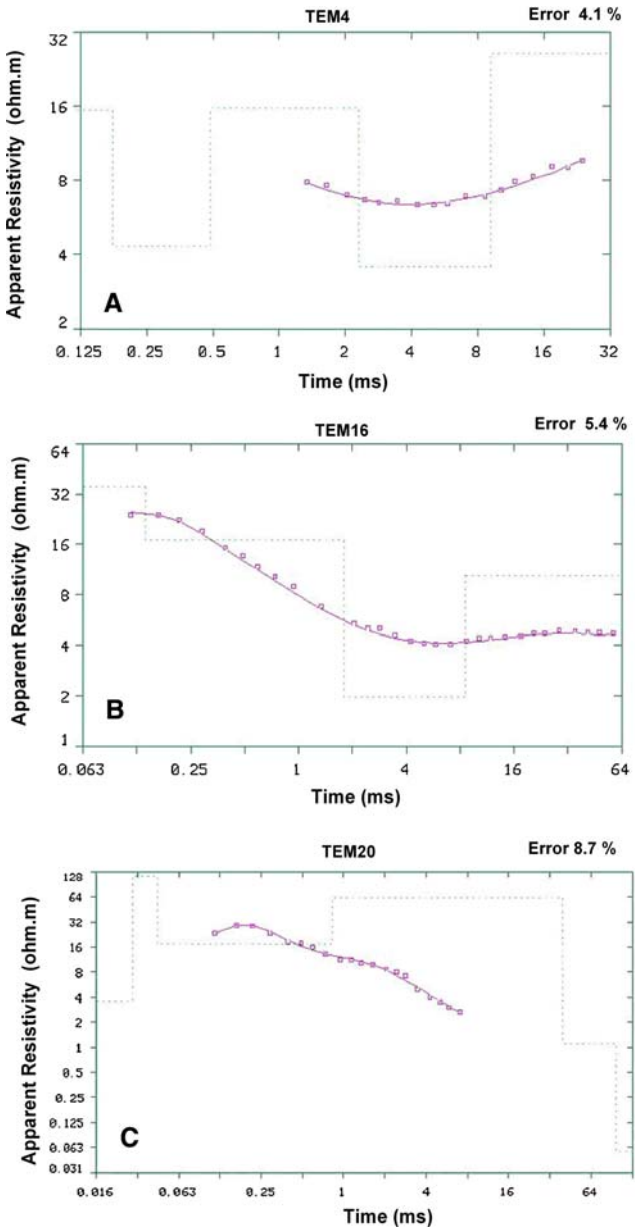

Fig. 8 Data and interpretation of three TEM 4 (A), 16 (B) and 20 (C). RMS 4, 5 and 9%, respectively

distances according to the following relation proposed by Meju (2005),

$$L = 711.8\,(t\rho)^{1/2} \quad (1)$$

L is in meters, t is the time in seconds and ρ is the homogeneous subsurface resistivity (in Ωm). The resistivity of the first layer was considered for such transformation.

The static-shift multiplicative factor g was calculated through the following relation:

$$g = \rho_{\mathrm{TEM}}/\rho_{\mathrm{VES}} \quad (2)$$

where ρ_{TEM} and ρ_{VES} are the TEM and VES apparent resistivities, respectively, for a common L.

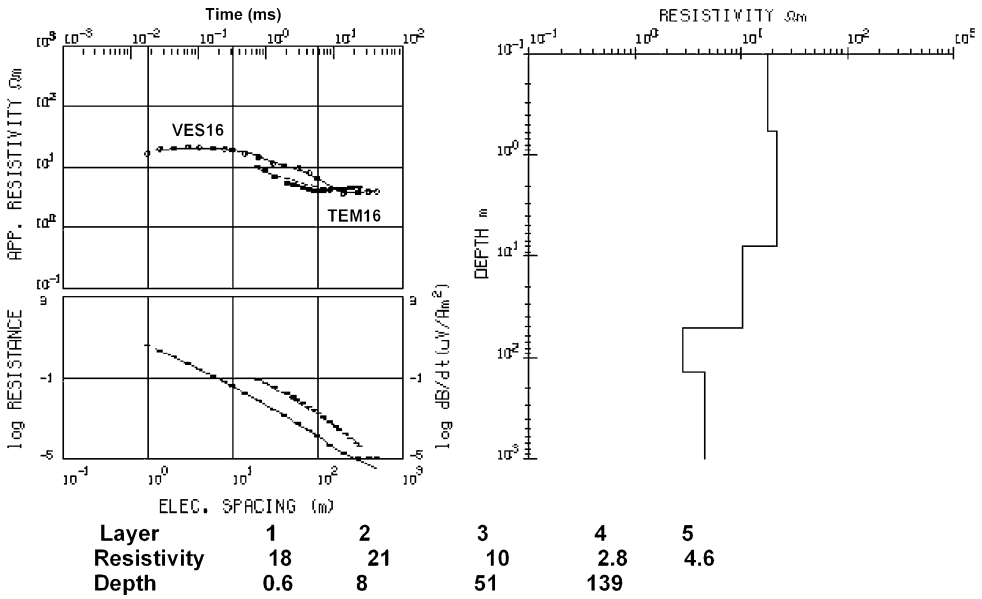

Fig. 9 Example of a joint inversion result (site 16)

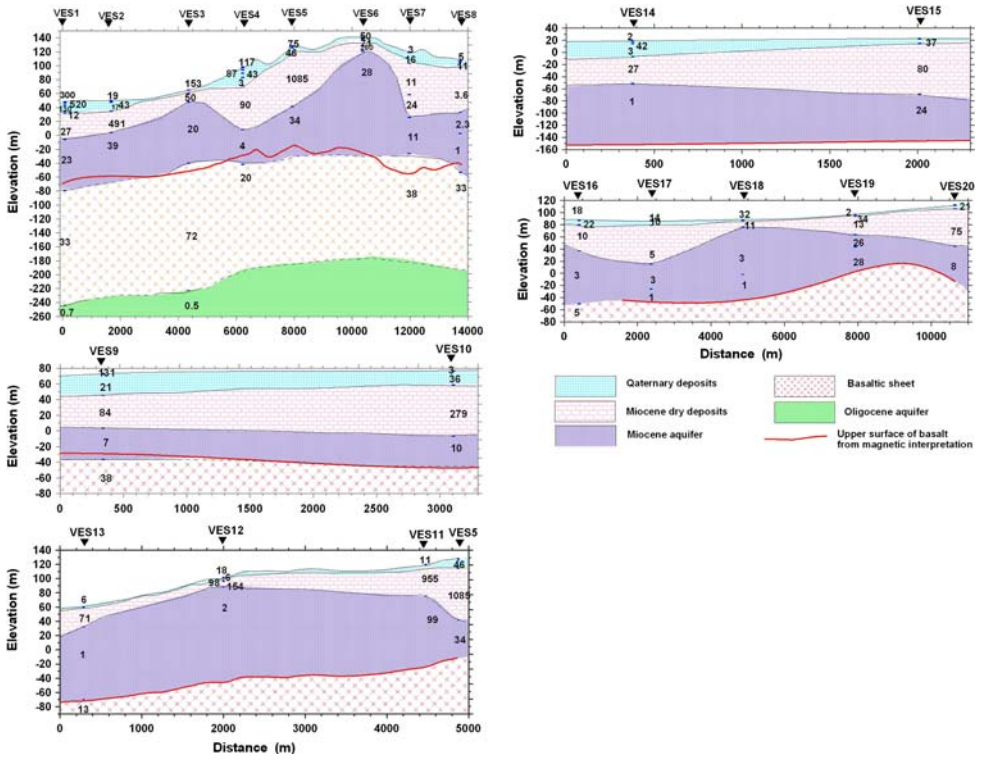

Fig. 10 Geoelectrical cross-sections from joint inversion of VES and TEM

The joint inversion of VES and TEM data was undertaken using Meju's code (DCEMINT, Version 2000). The results of the joint inversion (Fig. 10) were used in construction of the geoelectrical cross-sections showed in Fig. 11.

The results of the interpretation allowed characterizing five geoloelectric units (Table 1). The first unit (corresponding to the Quaternary deposits) is represented by the uppermost layer showing resistivity values varying from 2 to 520 ohm-m, according to the geological composition: the low resistivity values refer to mud and Nile silt and high resistivity value are associated to sand sheet and sand dunes. The second unit (representing dry Miocene deposits) that corresponds to the second layer shows a large variation in resistivity values (4–1,085 ohm-m) due to geological composition which consists of clay, sandy clay, marly limestone and limestone. The third layer is associated to the Miocene aquifer, which exhibit low resistivity

values. The fourth unit (related to the Oligocene basaltic sheet) is represented for the fourth layer which exhibits moderate resistivity values. The last layer represents the Oligocene aquifer, which is revealed as a very conductive layer due to the high salinity of the water, and detected at the VES1 and VES 3 only.

The increasing of the resistivity values associated with the Miocene aquifer at the eastern and western parts of the area may reflect a decreasing on the salinity of the water. Northern and southern parts of the aquifer show very low resistivities that might be related to an increasing of the salinity.

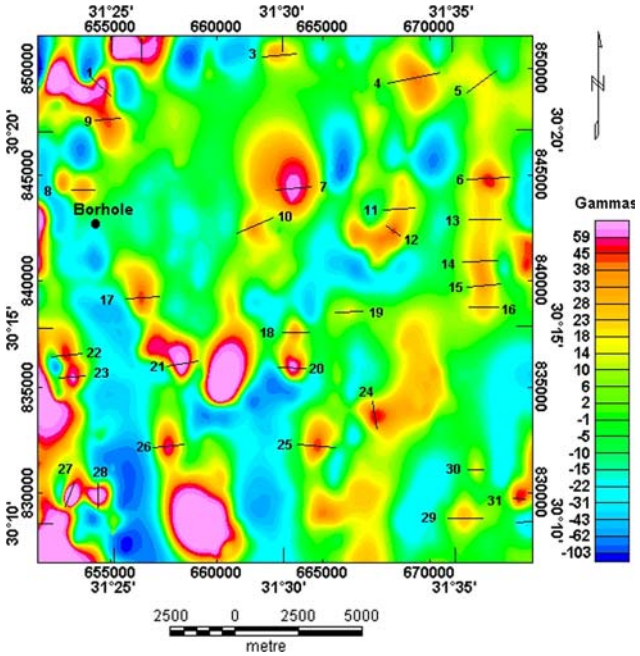

Fig. 11 Residual total intensity magnetic map reduced to the pole. Shown are the magnetic profiles whose interpretation is shown in Fig. 12

Table 1 Main geoelectric characteristics of the geological units from VES/TEM data joint inversion

Geological unit	Resistivity range (ohm-m)	Thickness range (m)	Conductance (Sm)
Quaternary deposits	2–520	1–28	0.5–0.0538
Miocene deposits	4–1,085	9.6–73	2.4–0.0673
Miocene (aquifer)	1–99	30–102	30–1.030
Oligocene (basaltic sheet)	5–72	165–183	33–2.54
Oligocene (salty aquifer)	0.5–0.7	–	

Magnetic data

A total of 871 land magnetic stations were measured covering the study area. The total magnetic field was measured using two Envimag proton magnetometers: one was used to record the magnetic field at one place (base station) in order to correct the diurnal variation of the magnetic field and the second instrument was used for field measurements. The measured data have been corrected of diurnal variation and IGRF.

The corrected data were contoured to obtain the total intensity magnetic map. The total intensity magnetic map was reduced to the magnetic pole to minimize the distortions of the magnetic field originated by the inclination and declination of the earth's field (Baranov 1957). The low and high pass filter technique has been applied on the RTP values to filter the regional and residual components (Fig. 12).

The results obtained from the modeling of 31 magnetic anomalies displayed in the residual map, were used to estimate the depth and the half width of the basaltic sheet. The modeling was performed with the Geosoft program (1994) and assuming a magnetic susceptibility of 0.00765 cgs unit. Figure 1 shows some of the interpreted anomalies. The results of the interpretation are summarized in the Table 2.

The results of the interpretation have been used to construct the depth map of the upper surface of the basalt sheet (Fig. 13). This map reveals that the basalt sheet is deeper (250 m) in the northwestern part of the area and shallow in the southeastern part (70 m) of the survey area. The results of magnetic interpretation were compared with result of borehole where the borehole gives 113.5 and depth map from magnetic has 105 m. The error = (113.5–105)/113.5 = 4.1%.

Conclusions

This work combined the interpretation of two complementary methods, magnetic and resistivity/TEM, as an effective approach to characterize groundwater reservoirs. The results obtained from magnetic survey in the vicinity of a well are compatible with the results from the geological log. The depth of the top of the basaltic sheet was observed at a depth of 113.5 m and interpreted, from magnetic data, at a depth of 105 m. The results obtained in the whole survey area can be considered as compatible with the results of the magnetic interpretation (Fig. 10). The Miocene aquifer was revealed as 30–102 m thick layer with a resistivity varying between 1 and 99 ohm-m. The Oligocene aquifer exhibits very low resistivity values (<1 ohm-m). The hydrochemistry of the water samples

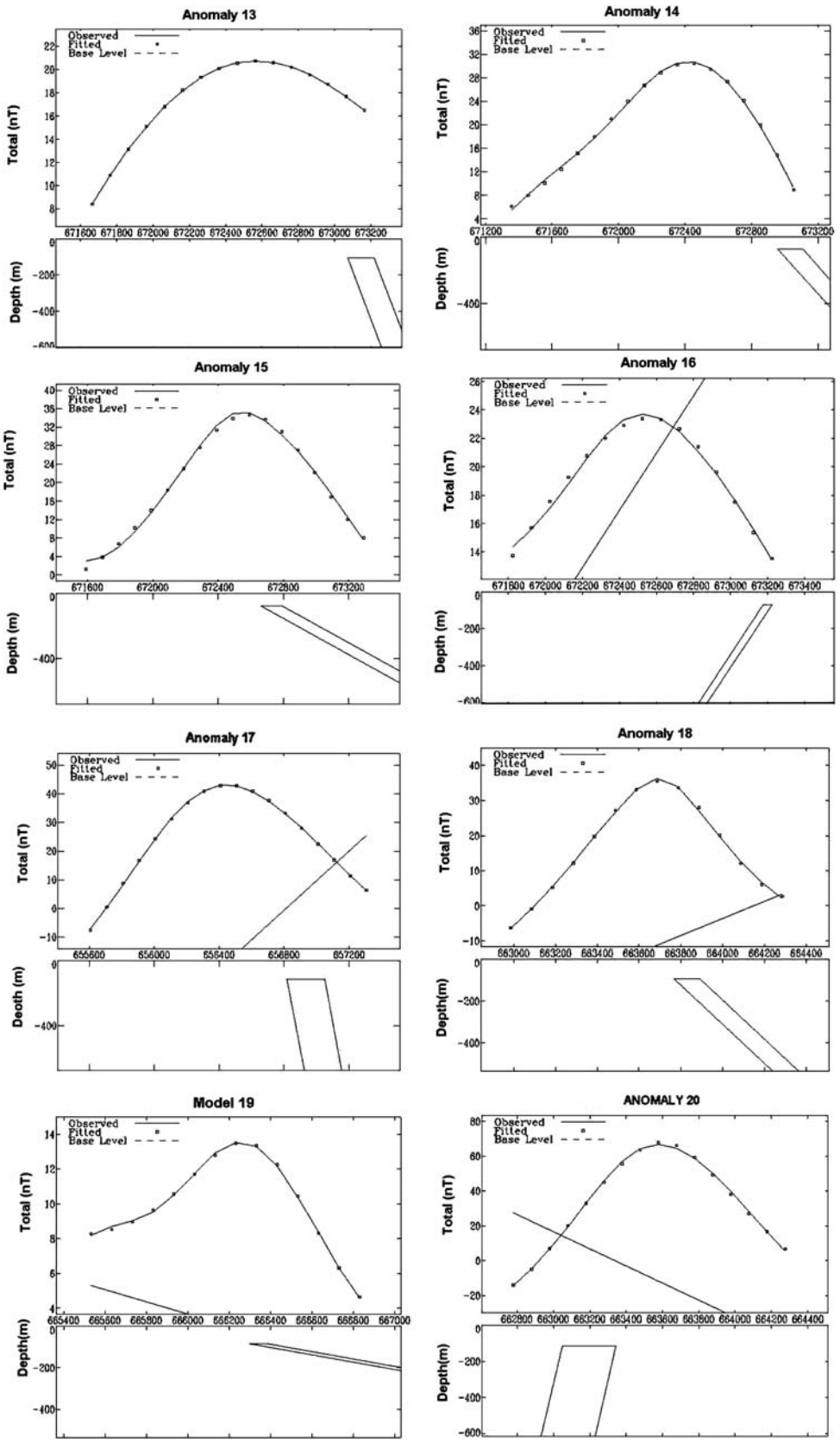

Fig. 12 Magnetic anomaly interpretation for anomalies 13–20

Table 2 Summary of the magnetic data modeling

Anomaly no.	Depth (m)	Half Width (m)	Anomaly no.	Depth (m)	Half Width (m)
1	261	361	17	113	116
2	177	296	18	92.4	62.5
3	173	257	19	84.1	43.9
4	218	253	20	114	148
5	84.1	37.7	21	126	157
6	127	101	22	101	113
7	127	123	23	77.9	96.2
8	100	45.4	24	215	424
9	156	143	25	141	150
10	183	176	26	99	112
11	165	79.2	27	135	114
12	194	866	28	192	357
13	106	73	29	107	73.8
14	69.5	75.5	30	121	44.5
15	80	66.2	31	240	34.8
16	70.5	23.7			

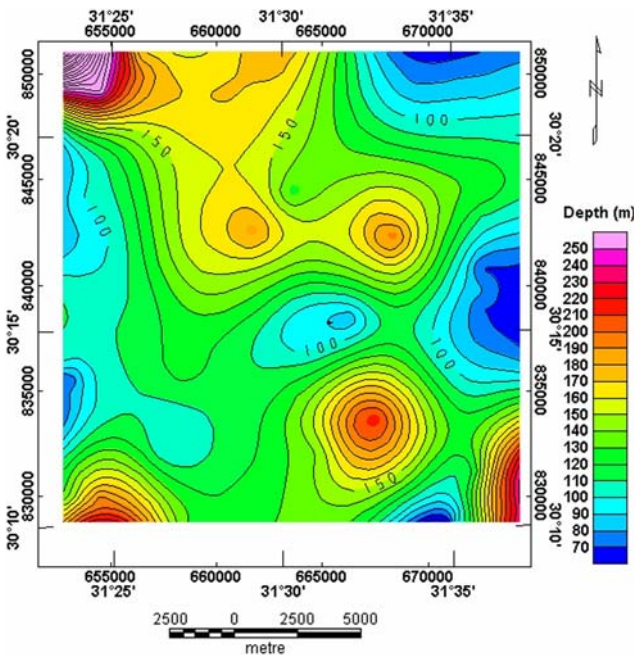

Fig. 13 Map of the top of the basaltic sheet obtained from the interpretation of the land magnetic data

from the borehole indicate that the TDS is 2,000 ppm in a sandy clay lithology.

Acknowledgments The first author is indebted to the Fundação para a Ciência e Tecnologia (Portugal) for his support through the post-doctor fellowship of reference (SFRH\BPD\22116\2005.

References

Baranov V (1957) A new method for interpretation of aeromagnetic maps: pseudo-gravimetric anomalies. Geophysics 22:359–383

Barker RD (1981) The offset system of electrical resistivity and its use with a multicore cable. Geophys Prospect 29:128–143

Barsukov PO, Fainberg EB, Khabensky EO (2004) Joint inversion of TEM and DC soundings, Near Surface. 10th European Meeting of Environmental and Engineering Geophysics, Utrecht, The Netherlands

Ebraheem AM, Sensosy MM, Dahab KA (1997) Geoelectrical and hydro-geochemical studies for delineating ground-water contamination due to salt-water intrusion in the northern part of the Nile delta, Egypt. Ground Water 35:216–222

Fitterman DV, Stewart MT (1986) Transient electromagnetic sounding for groundwater. Geophysics 51:995–1005

Flathe H (1955) Possibilities and limitations in applying geoelectrical methods to hydrogeological problems in the coastal areas of North West Germany. Geophys Prospect 3:95–110

Geological Survey of Egypt (EGSMA) (1998) Geology of Inshas area. Geological Survey of Egypt, internal report

Goldman M, Du Plooy A, Evkard M (1994) On reducing ambiguity in the interpretation of transient electromagnetic sounding data. Geophys Prospect 42:3–25

Interpex Limited (1995) TEMIX/XL Version 4, serial 4000, Interpex limited, Interpex House, 715, 14th street, PO Box 839, Colorado, USA

IPI2Win-1D Program (2000) Programs set for 1-D VES data interpretation. Department of Geophysics, Geological Faculty, Moscow University, Russia

McNeill JD (1990) Use of electromagnetic methods for groundwater studies. In:Ward SH (ed) Geotechnical and environmental geophysics, vol 1. Review and Tutorial, Society of Exploration Geophysicists Investigations, no 5, pp 107–112

Meju MA (2005) Simple relative space-time scaling of electrical and electromagnetic depth sounding arrays: implications for electrical static shift removal and joint DC-TEM data in version with the most-squares criterion. Geophys Prospect 53(4):463–480

Sharma SP, Baranwal VC (2005) Delineation of groundwater-bearing fracture zones in a hard rock area integrating very low frequency electromagnetic and resistivity data. J Appl Geophys 57:155–166

Urish DW, Frohlich RK (1990) Surface electrical resistivity in coastal groundwater exploration. Geoexploration 26:267–289

Van Overmeeren RA (1989) Aquifer boundaries explored by geoelectrical measurements in the coastal plain of Yemen: a case of equivalence. Geophysics 54:38–48

Zohdy AAR (1969) The use of Schlumberger and equatorial soundings in ground water investigations near El Paso, Texas. Geophysics 34:713–728